



Subtropical Mode Water in a recent persisting Kuroshio large-meander period: part II—formation and temporal evolution in the Kuroshio recirculation gyre off Shikoku

Hatsumi Nishikawa¹ · Eitarou Oka¹ · Shusaku Sugimoto²

Received: 9 November 2022 / Revised: 20 February 2023 / Accepted: 29 March 2023 / Published online: 12 April 2023
© The Author(s) 2023

Abstract

Since August 2017, the large meander (LM) path of the Kuroshio south of Japan has continued to date for more than five years, with a local Kuroshio recirculation gyre off Shikoku (RGOS). The formation and temporal evolution of Subtropical Mode Water (STMW) in the isolated RGOS were examined by using Argo profiling float and shipboard observation data. Since the late winter of 2018, which was the first winter of the current LM event, multiple STMW layers with different densities overlapping with each other have been observed for more than three years inside the RGOS. The deeper STMW layer of 18.0 °C, which was formed in the late winter of 2017 before the current LM event began, has survived at least until September 2021 while its thickness and horizontal extent has decreased gradually. We may have succeeded in discovering the longest survived STMW ever observed due to a suitable environment for STMW conservation inside the RGOS. On the other hand, the shallower STMW layer(s) of 19.0–19.8 °C, which was originally formed over the deeper STMW layer in the late winter of 2018, has been repeatedly renewed or dissipated in the following years. The oxygen utilization rate at the core of the deeper STMW at a depth of 500 dbar was estimated to be 4.6 $\mu\text{mol kg}^{-1} \text{ yr}^{-1}$, which is believed to be explained solely by oxygen consumption due to remineralization.

Keywords North Pacific Subtropical Mode Water · Kuroshio large meander · Recirculation gyre off Shikoku · Oxygen utilization rate

1 Introduction

The North Pacific Subtropical Mode Water (STMW; Masuzawa 1969), which is characterized by a thick thermostad with a potential temperature (θ) between 16 and 19.5 °C (Oka 2009), is formed as deep winter mixed layers (ML) south of the Kuroshio and Kuroshio Extension and north of 28°N (Suga and Hanawa 1990; Oka and Suga 2003). The colder variety of STMW with $\theta = 16 - 18$ °C, which accounts for more than 80% of the total STMW volume, is formed east of 140°E, i.e., south of the KE, while the warmer variety of STMW with $\theta = 18 - 19.5$ °C is formed mainly south of the Kuroshio to

the west of 140°E (Oka et al. 2021). After formation, both varieties are advected southwestward by the mean flow in the southern part of the Kuroshio recirculation gyre (Suga and Hanawa 1995a) and by mesoscale eddy activity (Uehara et al. 2003; Nishikawa et al. 2010; Xu et al. 2016) to spread as far as 20°N to the south and just east of Taiwan to the west within 2–3 years (Oka 2009). STMW transmits signals resulting from air-sea interaction such as temperature anomalies to the ocean subsurface through its subduction process (Yasuda and Hanawa 1997; Oka and Qiu 2012; Newman et al. 2016). These anomalies then reappear at the sea surface in the formation region (Hanawa and Sugimoto 2004) or in a remote area (Sugimoto and Hanawa 2005), possibly affecting atmosphere.

The formation and advection of STMW are significantly affected by the Kuroshio path variations south of Japan among three typical paths: the large meander (LM) path and the offshore and nearshore non-large-meander (NLM) paths (Fig. 1; Kawabe 1995). When the Kuroshio takes an LM path, the westward advection of the colder variety of STMW formed east of 140°E is inhibited, drastically reducing its volume on

✉ Hatsumi Nishikawa
hatsu.nishikawa@aori.u-tokyo.ac.jp

¹ Atmosphere and Ocean Research Institute, The University of Tokyo, Kashiwa 277-8564, Japan

² Department of Geophysics, Graduate School of Science, Tohoku University, Aoba-Ku, Sendai 980-8578, Japan

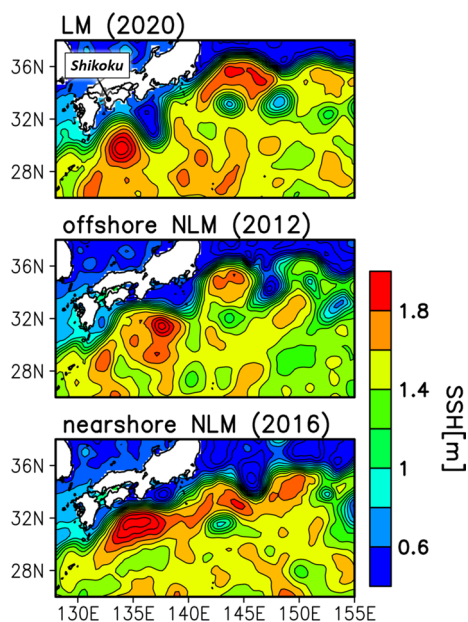


Fig. 1 Sea surface height (SSH) maps in March of 2020 (top), 2012 (middle), and 2016 (bottom) corresponding to the periods of the LM, offshore NLM, and nearshore NLM paths of the Kuroshio, respectively

the western side of the LM (Suga and Hanawa 1995a, b; Oka et al. 2021). In addition, when the Kuroshio takes a meandering path (i.e., LM and offshore NLM paths), the warm STMW exceeding 19 °C is formed in the local Kuroshio's recirculation gyre off Shikoku (RGOS), which is separated from the recirculation gyre south of the KE and isolated to the southwest of the meandering path of the Kuroshio (Nishiyama et al. 1980, 1981; Oka 2009; Sugimoto and Hanawa 2014; Fig. 1). By using Argo profiling float data from 2005 to 2011, Sugimoto and Hanawa (2014) showed a double-layer structure of STMW in the isolated RGOS, which composed of the warmer STMW exceeding 19 °C developed in the RGOS and the colder one formed east of 140°E in previous winters and advected from there. However, each meandering path event during 2005–2011 (i.e., the LM event in 2005 and offshore NLM events in 2007 and 2009) lasted for less than one year, and the behaviors of STMWs in the isolated RGOS over multiple years have remained unclear.

In August 2017, the Kuroshio LM occurred 12 years after the previous event in July 2004–August 2005, and has continued to date (as of February 2023), which is the longest record in the observation history since 1950 (Qiu and Chen 2021). This is also the first multi-year LM event in the era of satellite altimeter and Argo, which enabled us to investigate water mass processes in relation to currents and mesoscale eddies in detail. To clarify the formation and temporal evolution of STMW in the isolated, multi-year RGOS, we analyze Argo profiling floats, satellite-derived altimeter data, and

shipboard observations in this paper. Section 2 explains the data and the analysis method. Section 3 describes the STMW structure and its time evolution in the RGOS observed by Argo float and shipboard observations. Section 4 discusses the estimated oxygen utilization rate in the STMW. Finally, Sect. 5 gives our summary.

2 Data and method

We used temperature (T) and salinity (S) profiles from Argo floats inside the RGOS in 2017–2021, which were downloaded from the ftp site of the Argo Global Data Assembly Center (<ftp://usgodae.org/pub/outgoing/argo>, <ftp://ftp.ifremer.fr/ifremer/argos>, <https://doi.org/10.17882/42182>) and edited as outlined in Oka et al. (2007). Each profile was vertically interpolated onto a 1-dbar grid using the Akima spline (Akima 1970). To obtain vertical cross sections in the RGOS, we averaged profiles in every 10-km bin from the RGOS center, which is detected as the highest sea surface height (SSH) from satellite altimeter (detailed below). We also used T , S , and dissolved oxygen profiles from two research cruises. The first one is observations by a conductivity-temperature-depth profiler (CTD) with a RINKO rapid-response dissolved oxygen sensor and expendable bathythermograph (XBT) across the RGOS, which were conducted in 16–17 June 2018 in the KS1805 cruise of *R/V Keifu-maru* by the Japan Meteorological Agency. Since XBT only measures T , we estimated S from XBT T profile based on the T – S relationship obtained from CTD (Stommel 1947; Goes et al. 2018). The second one is intensive shipboard observations during 28–29 May 2021 in the KS-21–9 cruise of the *R/V Shinsei-maru* that we carried out to explore the STMW in the RGOS. T and S profiles were obtained at intervals of 10 min in latitude and longitude crossing the RGOS meridionally and zonally by expendable CTD (XCTD). T , S , and dissolved oxygen profiles near the center of the RGOS were also obtained by a conductivity-temperature-depth-oxygen profiler (CTDO₂).

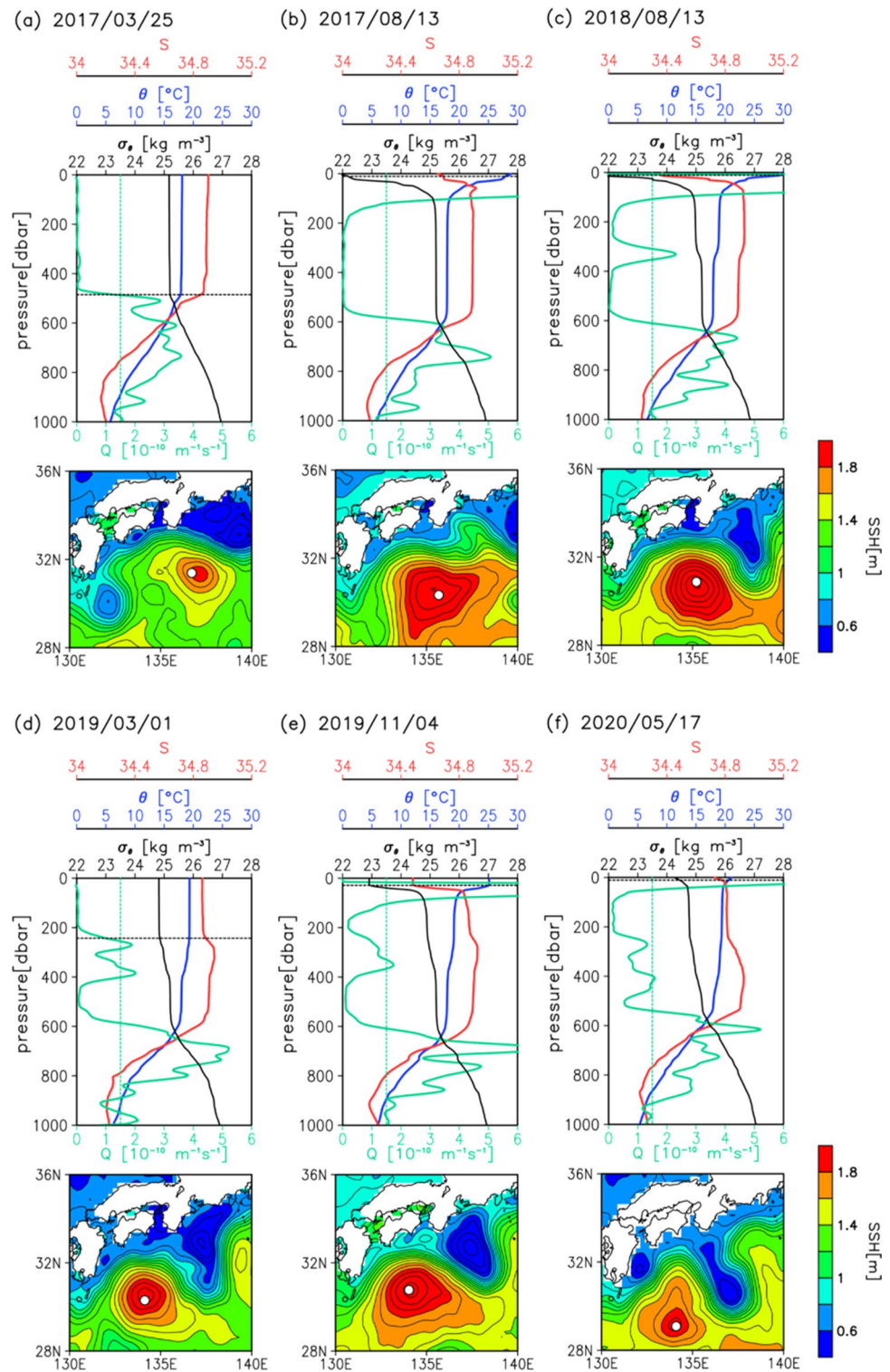
We calculated θ , potential density (σ_θ), and potential vorticity (Q) from the Argo and shipboard T/S profiles. Here, Q is defined as $Q = gf\partial\sigma_\theta/\partial p$, neglecting relative vorticity (Qiu et al. 2006), where g is the gravity acceleration, f is the Coriolis parameter, and p is pressure. STMW was detected as layers with $Q < 1.5 \times 10^{-10} \text{ m}^{-1} \text{ s}^{-1}$ and $\theta = 16\text{--}20.5 \text{ }^\circ\text{C}$. The core of STMW was defined as a local vertical minimum of Q in each profile. We defined mixed layer depth as the depth at which σ_θ increases by 0.03 kg m^{-3} from its 10-dbar depth value (Boyer Montégut et al. 2004; Oka et al. 2007). After the saturated dissolved oxygen concentrations were estimated for each depth from the observed T and S (Weiss 1970), apparent oxygen utilization (AOU) was computed as

the difference between the saturated and observed dissolved oxygen concentrations.

To assess conditions of the Kuroshio and the RGOS and detect the RGOS center, the absolute SSH data from the satellite altimeter, Global Ocean Gridded Level 4 Sea Surface

Heights (<https://doi.org/10.48670/moi-00148>, <https://doi.org/10.48670/moi-00149>), produced and distributed by the Copernicus Marine and Environment Monitoring Service (CMEMS; <http://marine.copernicus.eu>), were also used. The

Fig. 2 Vertical profiles of Q (green), S (red), θ (blue), and σ_θ (black) obtained by Argo floats (upper panels) on **a** 25 March 2017, **b** 13 August 2017, **c** 13 August 2018, **d** 1 March 2019, **e** 4 November 2019, and **f** 17 May 2020 at the position indicated by a white dot in the SSH maps (lower panels). In the upper panels, vertical green dashed line denotes $Q = 1.5 \times 10^{-10} \text{ m}^{-1} \text{ s}^{-1}$, while horizontal black dashed line represents the mixed layer depth



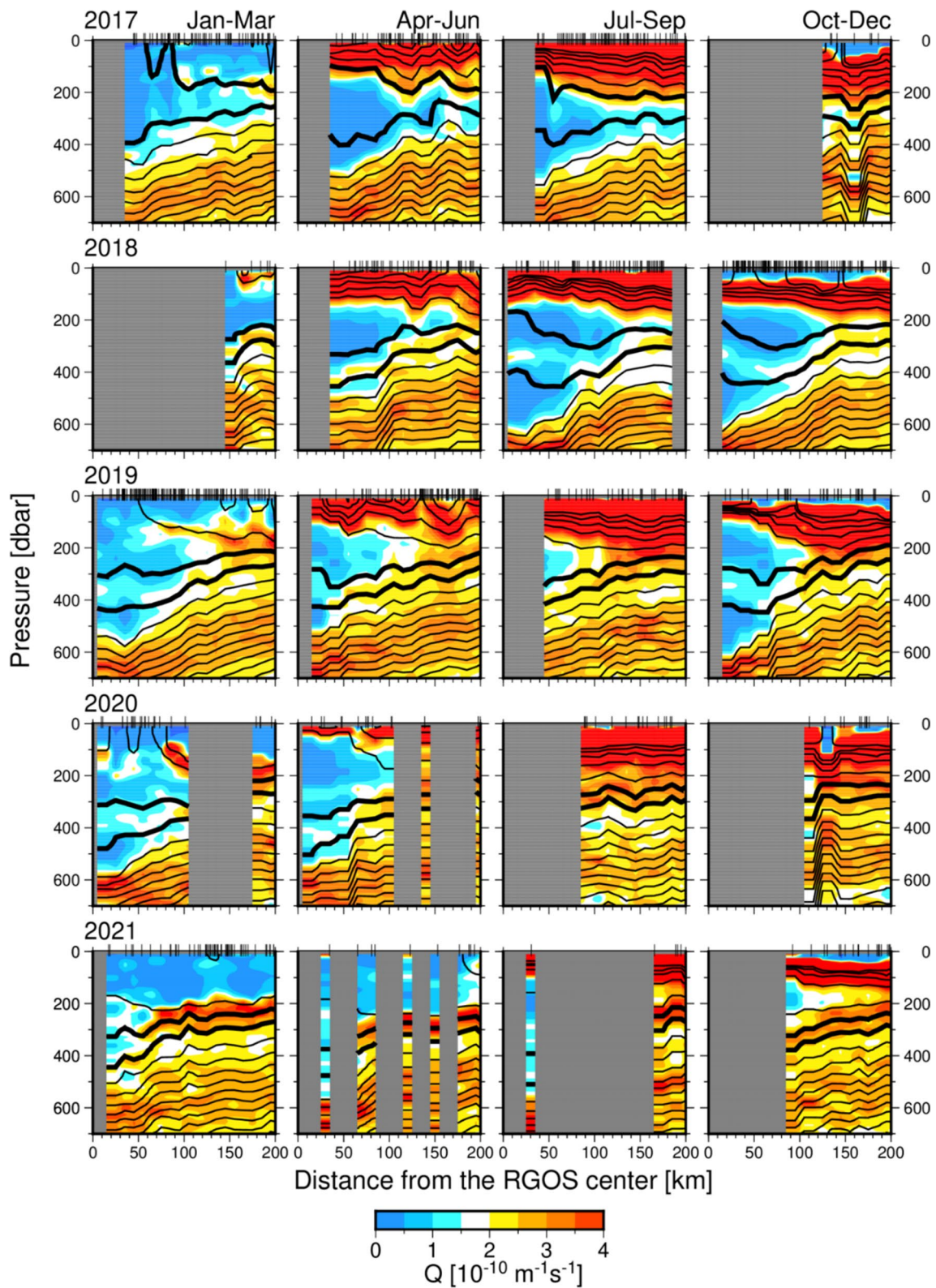


Fig. 3 Vertical cross sections of Q (color) and θ (contour) composited from data by averaging Argo profiles every 10 km in each season from 2017 to 2021. Horizontal axis indicates the distance from

the RGOS center. Contour interval for θ is 1 °C. Thick contours show 18 °C and 19 °C isotherms. Bars at the top of the panels indicate location of Argo floats

data are available at daily temporal and $0.25^\circ \times 0.25^\circ$ spatial resolutions.

3 Temporal evolution of STMW structure and long survival of deeper STMW in the RGOS

In late March 2017 before the current LM began, the Kuroshio took an offshore NLM path, and the RGOS was being established (SSH map in Fig. 2a). An Argo float located

near the center of the RGOS in formation observed a deep winter mixed layer approaching 500 dbar with $\theta = 18.0^\circ\text{C}$, $S = 34.89$, and $\sigma_\theta = 25.18 \text{ kg m}^{-3}$ (Fig. 2a), which were close to the properties of the colder variety of STMW formed south of the Kuroshio Extension (Oka et al. 2021). In August 2017 when the current LM began, a vertically uniform STMW layer with a core θ of 17.9°C , a core S of 34.89, and a core σ_θ of 25.21 kg m^{-3} was found in the subsurface at depths of 150–600 dbar (Fig. 2b). From April to September of 2017, the STMW layer existed over 200 km from the RGOS center with a maximum thickness of 400 dbar

Fig. 4 **a** Locations of CTD (white circle) and XBT (black cross) stations in the KS1805 cruise. Black contours with color denote SSH on 16 June 2018. **b–d** Cross sections of **(b)** Q , **(c)** θ , and **(d)** σ_θ along the observation line indicated in (a). The “v” symbols in black and red indicate XBT and CTD observation points, respectively

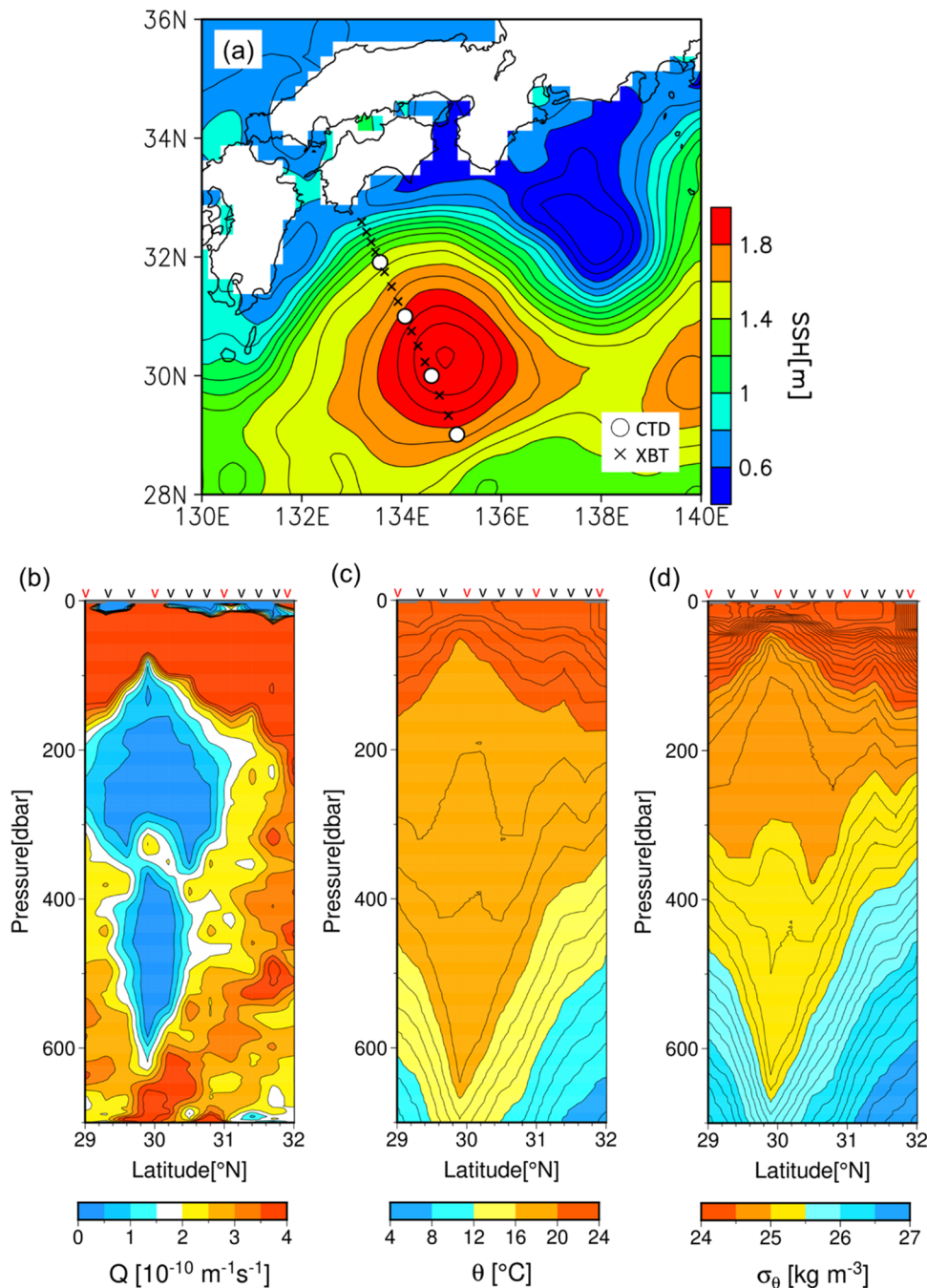


(Fig. 3). Hereafter, the STMW formed in the late winter 2017 is referred to as the STMW-2017, and STMWs formed in other years are also denoted in the same manner.

While Argo floats were not distributed near the center of the RGOS from fall of 2017 to spring of 2018 (Fig. 3), shipboard observations conducted in June 2018 captured a double layer structure of STMW across the RGOS (Figs. 4 and 5). The shallower STMW layer at depths of 100–300 dbar with a width of 200 km had a core θ of 19.0 °C, a core S of 34.93, and a core σ_θ of 24.98 kg m⁻³, while the deeper STMW layer at 350–620 dbar with a width of 100 km had a core θ of 18.0 °C, a core S of 34.89, and a core σ_θ of 25.20 kg m⁻³. The deeper STMW layer is believed to be formed in the previous year because the water properties are almost the same with those of the STMW-2017 (Fig. 2a, b). Therefore, the shallower STMW layer was probably formed in the late winter of 2018 (STMW-18). STMW-2018 was warmer than STMW-2017 by 1 °C, having properties close to the warmer variety of STMW formed south of Japan (Oka et al. 2021). The double STMW layers were also observed by an Argo float at depths of 100–300 and 350–600 dbar in August 2018 (Fig. 2c). The shallower and deeper STMW were distributed up to 150 km and 90 km from the RGOS center in the summer of 2018, respectively (Fig. 3). Such a double STMW layer structure was maintained until the end of 2018 while their horizontal extent gradually decreased.

Similar multiple structure of STMW has been frequently observed (e.g., Taneda et al. 2000; Oka et al. 2011; Liu et al. 2017). The earlier study inferred that the multiple structure south of the Kuroshio Extension was formed due to interleaving of STMWs with slightly different densities (Oka et al. 2011). A shipboard survey in the western North Atlantic observed pronounced double STMW layers with a core θ difference of 1.7 °C, which were formed due to the vertical alignment of two warm-core rings with low- Q water pinched off from the Gulf Stream meander (Belkin et al. 2020). On the other hand, profiling float observations in the western North Pacific revealed that in a westward propagating anticyclonic eddy, a warmer STMW was formed south of Japan, overlying a colder STMW formed in the region south of the KE and advected from there within the eddy (Xu et al. 2017; Liu et al. 2019). Such formation of multiple layers was similar to that in the RGOS.

In early March 2019 (Fig. 2d), the upper part of the STMW-2018 was entrained into the winter mixed layer that developed down to a depth of 240 dbar, and new STMW, i.e., STMW-2019, was being formed in the mixed layer, establishing a triple STMW layer structure. The θ , S , and σ_θ of the winter mixed layer, i.e., shallow STMW layer in progress of formation, were 19.4 °C, 34.86, and 24.83 kg m⁻³, respectively (Fig. 2d). The core θ , S , and σ_θ of middle and deep STMW layers at depths of 309 and 493 dbar were 19.0 °C, 34.94, and 24.98 kg m⁻³, and 18.0 °C, 34.91, and

25.21 kg m⁻³, which were almost the same as those of the STMW-2018 and STMW-2017, respectively. In November 2019, the core of the middle STMW-2018 was mostly disappeared, and the double STMW layer structure was again established inside the RGOS (Fig. 2e). The shallow STMW-2019 had a core θ of 19.1 °C, a core S of 34.87, and a core σ_θ of 24.90 kg m⁻³. The deep STMW-2017 with a core θ of 17.9 °C, a core S of 34.90, and a core σ_θ of 25.21 kg m⁻³, the thickness and radius of which is about 250 dbar and 70 km, was well preserved within the RGOS, although it was difficult to see in the summer 2019 due to lack of profiles near the RGOS center (Fig. 3).

In May 2020, triple STMW layers consisting of the shallow STMW with a core θ , S , and σ_θ of 19.5 °C, 34.81, and 24.76 kg m⁻³, the middle STMW-2019 with 19.1 °C, 34.89, and 24.92 kg m⁻³, and the deep STMW-2017 with 18.0 °C, 34.91, and 25.20 kg m⁻³ were observed near the RGOS center (Fig. 2f). The shallow STMW was believed to be formed in the late winter 2020 (STMW-2020) as a result of the renewal of the upper part of the STMW-2019 by the entrainment into the winter mixed layer. The middle STMW-2019 had a thickness of 150 dbar and spread within 120 km from the RGOS center (Fig. 3). The deep STMW-2017 still

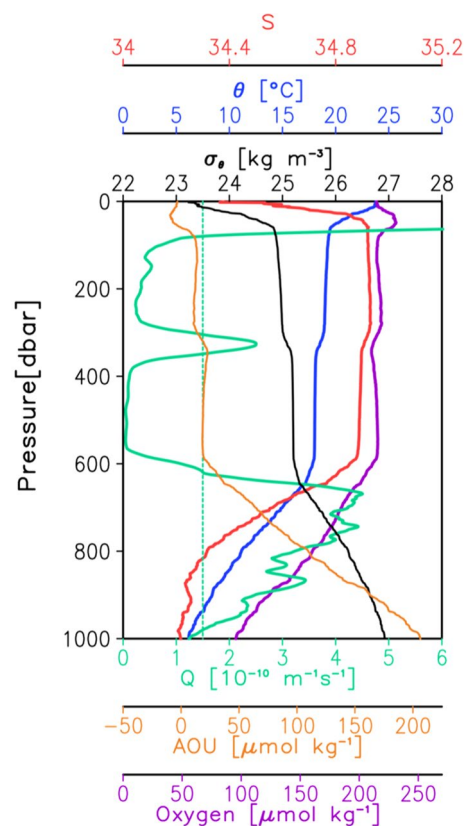


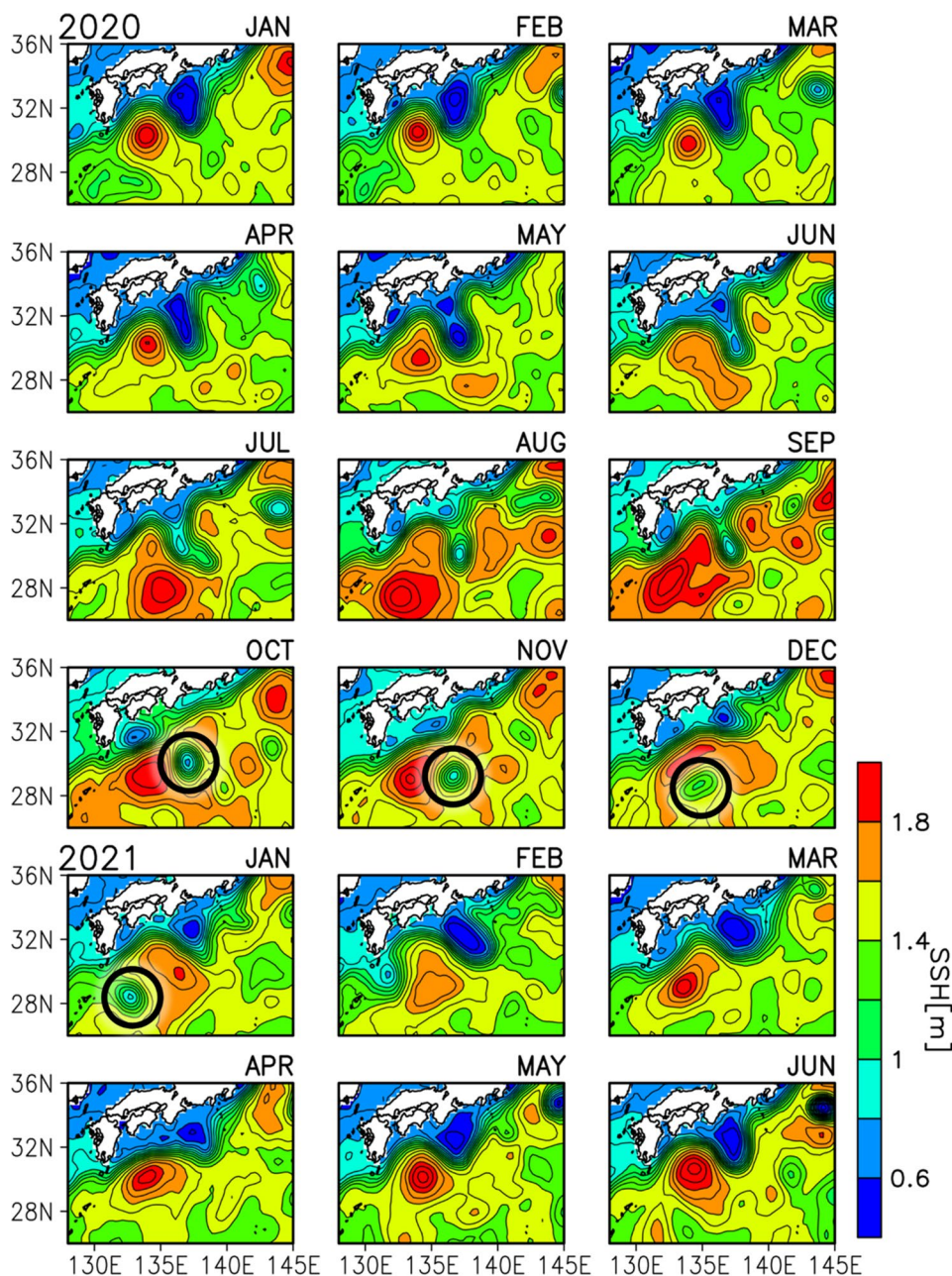
Fig. 5 Vertical profiles of Q (green), S (red), θ (blue), σ_θ (black), AOU (orange), and dissolved oxygen (purple) obtained at 30°N, 134.5°E on 16 Jun 2018 in the KS1805 cruise. Green dashed line denotes $Q = 1.5 \times 10^{-10} \text{ m}^{-1} \text{ s}^{-1}$

survived while its thickness and radius decreased to 100 dbar and 50 km, respectively (Figs. 2f and 3).

The Kuroshio LM became unstable after June 2020, detaching an intense cold eddy in October 2020 (Fig. 6). The detached cold eddy migrated westward for four months and merged with the Kuroshio south of Kyushu in February 2021 again. During the migration period, the RGOS was transformed significantly. How did such transformation influence the STMW structure in the RGOS, especially the deep STMW-2017? To observe the STMW structure after the RGOS deformation event, we carried out intensive CTDO₂ and XCTD observations during the KS-21-9 cruise of *R/V Shinsei-maru* in May 2021 (Figs. 7a), and succeeded in

observing triple STMW layers near the center of the RGOS (Figs. 7 and 8). The shallow STMW layer with a thickness of 250 dbar had a core θ of 19.8 °C, a core S of 34.82, and a core σ_θ of 24.67 kg m⁻³ at a depth of 247 dbar (Fig. 8). Although two PV minima were found at depth of 82 and 247 dbar within the shallow STMW layer, they were considered within the same layer because the water properties at each depth of PV minima were quite similar. As these properties were different from those of the STMW-2020, the shallow STMW layer must have been newly formed in the late winter 2021 (STMW-2021). The middle STMW layer at depths of 350–400 dbar had a core θ of 19.1 °C, a core S of 34.87, and a core σ_θ of 24.89 kg m⁻³, which agree with those of

Fig. 6 Monthly SSH maps south of Japan during a LM deformation period from January 2020 to June 2021. The detached cold eddy is enclosed by black circle



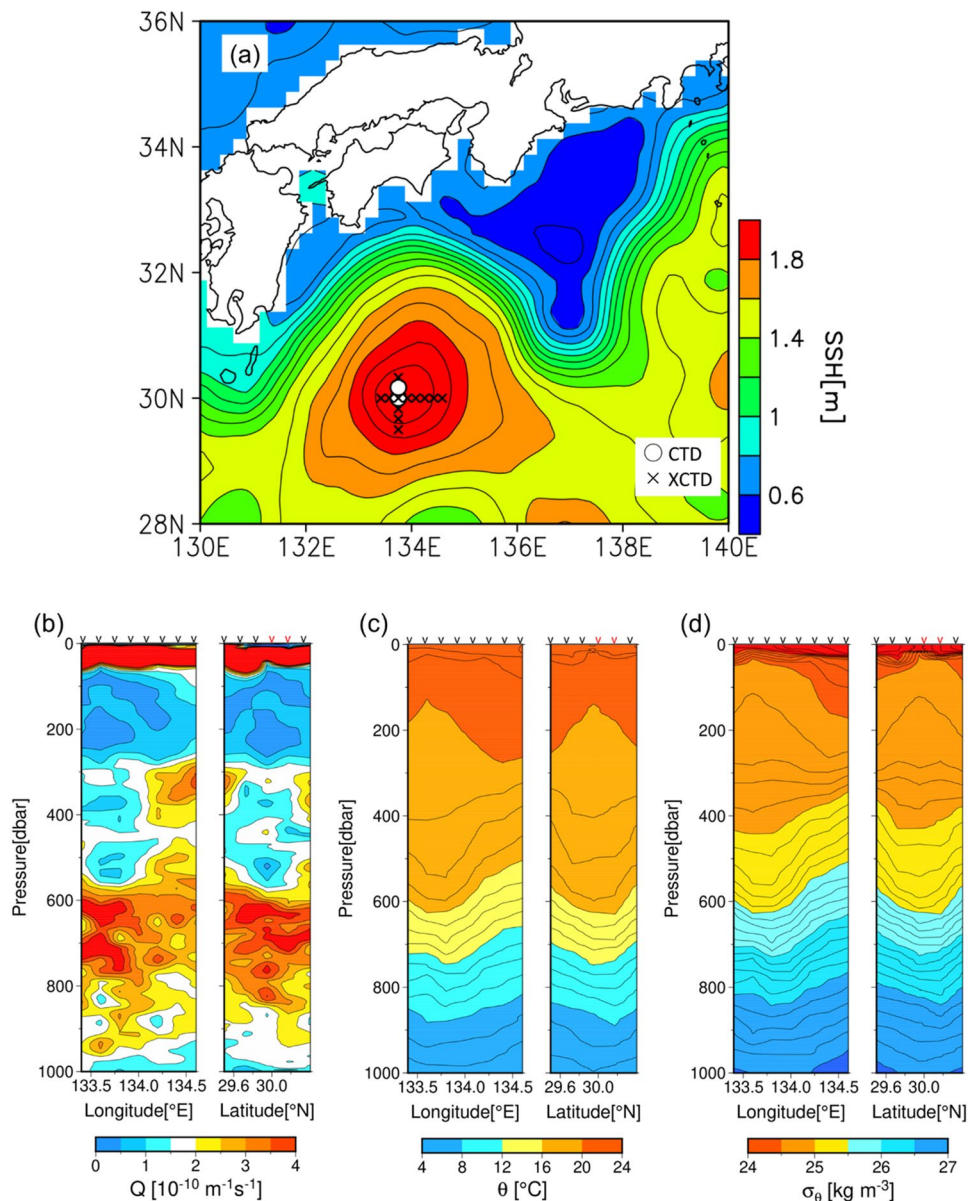
STMW-2019. The core properties of the deep STMW layer (18.0 °C, 34.87, and 25.18 kg m⁻³) were close to those of STMW-2017 (Fig. 2b). Thus, the STMW-2017 was found to survive for more than four years while its thickness and width had shrunk to 80 m and 40 km, respectively (Fig. 7). Furthermore, in September 2021, STMW with a core θ , S , and σ_θ of 17.9 °C, 34.84, and 25.18 kg m⁻³ at a depth of 522 dbar was captured by an Argo float located 30 km from the RGOS center (Figs. 3 and 9). Since these properties were also similar to those of STMW-2017, it is expected that STMW-2017 has survived until at least September 2021. Most of STMW reaches the western boundary in two years after its formation, and then the properties dissipate (e.g., Oka 2009). A series of results indicate that the isolated RGOS is a suitable environment for STMW conservation,

and we may have succeeded in observing the longest survived STMW.

4 Estimation of oxygen utilization rate

Time series observations of STMW-2017 in the RGOS for four years provide a unique opportunity to explore the oxygen utilization rate (OUR) in the ocean. AOU has been used to estimate the age of water masses (e.g., Suga et al. 1989; Oka and Suga 2005). It tends to increase in time due to the oxygen consumption through remineralization of organic matter after isolation of the water mass from the atmosphere (Jenkins 1980) and due to mixing with surrounding older water. OUR is an important indicator for biological

Fig. 7 **a** Locations of CTD (white circle) and XCTD (black cross) stations in the KS-21–9 cruise. Contours with color denote SSH on 29 May 2021. **(b–d)** Vertical cross section of **b** Q , **c** θ , and **d** σ_θ along the observation lines indicated in **(a)**. The “v” symbols in black and red indicate XCTD and CTD observation points



processes in the interior ocean, although it is difficult to precisely estimate OUR since oxygen concentrations also fluctuate due to physical processes such as mixing.

Fortunately, the STMW-2017 had been trapped within the RGOS and isolated from its surroundings as described in Sect. 3. The shipboard observation in June 2018 demonstrated that the core of the deeper STMW-2017 had an AOU of $18.4 \mu\text{mol kg}^{-1}$ and Q of $0.05 \times 10^{-10} \text{ m}^{-1} \text{ s}^{-1}$ at a depth of 545 dbar (orange curve in Fig. 5), while the shipboard observation in May 2021 showed that the core of the deep STMW-2017 had an AOU of $32.1 \mu\text{mol kg}^{-1}$ and Q of $0.348 \times 10^{-10} \text{ m}^{-1} \text{ s}^{-1}$ at a depth of 520 dbar (orange curve in Fig. 8). Since STMW-2017 observed in both 2018 and 2021 was characterized by a low core Q , it would be little affected by diffusion. Therefore, the AOU difference of $13.7 \mu\text{mol kg}^{-1}$ can be explained solely by oxygen consumption due to remineralization, and is divided by three years to yield an OUR of $4.6 \mu\text{mol kg}^{-1} \text{ yr}^{-1}$ at depth of 500 dbar. This OUR is consistent with those from previous works: $4.5 \mu\text{mol kg}^{-1} \text{ yr}^{-1}$ averaged at depths of 200–1000 m, which was derived from the observed AOU and the water age based on chlorofluorocarbons and ^{14}C in the western North Pacific by Feely et al. (2004), and $4.2 \pm 0.27 \mu\text{mol kg}^{-1} \text{ yr}^{-1}$ at depths of 100–500 m, which was estimated using water

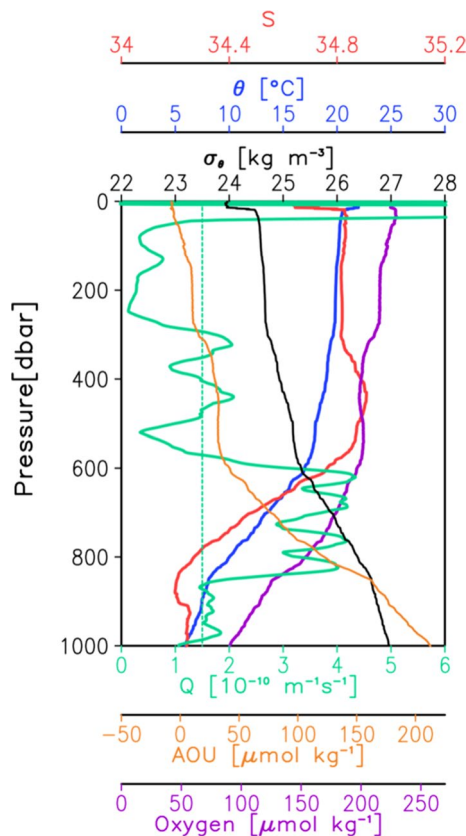


Fig. 8 Vertical profiles at 30 N, 133.75 E on 29 May 2021 in the KS-21-9 cruise, otherwise following Fig. 5

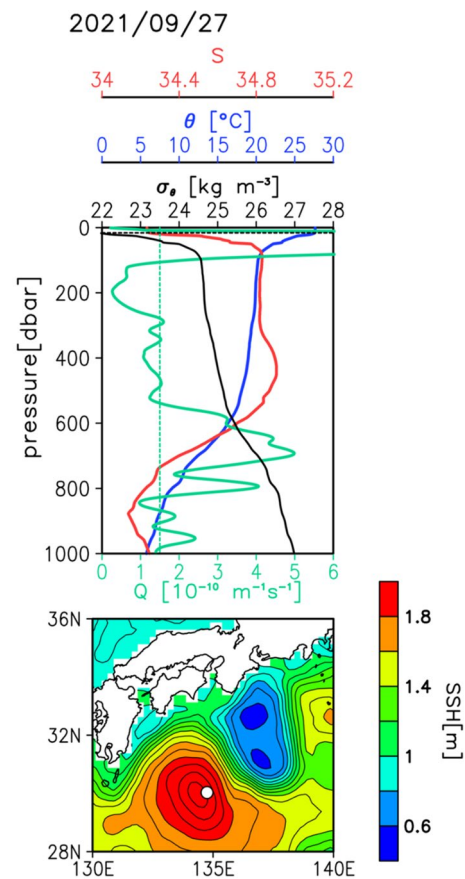


Fig. 9 Vertical profiles (upper panel) and the SSH map (lower panel) on 27 September 2021, otherwise following Fig. 2

age based on tritium and helium isotope observation in the South China Sea by Xie et al. (2021).

While most of previous OUR estimates, including those mentioned above, have relied on chemical tracers, Billheimer et al. (2021) recently succeeded in estimate of OUR using high resolution oxygen data from biogeochemical profiling floats deployed under the CLIVER Mode Water Dynamics Experiment (CLIMODE; Marshall et al. 2009) in the Sargasso Sea. They also clarified the depth dependence and seasonal variation of OUR, which are valuable for diagnosis of the carbon cycle in the Sargasso Sea. Currently, biogeochemical floats with an oxygen sensor are being expanded in the North Pacific region. Their data are expected to reveal the detailed spatial–temporal distribution and variability of OUR and contribute to our improved understanding of the carbon cycle in the North Pacific.

5 Summary

Argo floats and shipboard observation data in 2017–2021 were analyzed to investigate the formation and temporal evolution of STMW in the isolated RGOS during the current Kuroshio LM period that has lasted since August 2017. In the late winter of 2017 before the current LM event, when the Kuroshio took an offshore NLM path, vertically uniform STMW-2017 of 18.0 °C with a thickness of 500 dbar was formed in the RGOS. In the late winter of 2018, the upper part of the STMW-2017 was entrained into the winter mixed layer, which newly became STMW-2018 of 19.0 °C. Since then, the STMW inside the RGOS has maintained a multi-layer structure for more than three years. The shallower STMW layer(s) originated in 2018 was partially renewed or dissipated in the following years. The deeper STMW-2017 layer has survived at least until September 2021 for 4.5 years, while its thickness and width had shrunk, particularly due to the transformation of the RGOS in October 2020–February 2021 in association with the migration of intense cold eddy detached from the LM. We may have succeeded in observing the longest survived STMW due to a suitable environment for STMW conservation in the RGOS.

The core of STMW-2017 was observed to have AOU values of 18.4 $\mu\text{mol kg}^{-1}$ in June 2018 and 32.1 $\mu\text{mol kg}^{-1}$ in May 2021, which yielded an OUR of 4.6 $\mu\text{mol kg}^{-1} \text{yr}^{-1}$ at a depth of 500 dbar. This value agrees with previous estimates derived from chemical tracers, and is believed to be explained solely by oxygen consumption due to remineralization because the STMW had been trapped within the RGOS and little diffused.

The Kuroshio LM is still ongoing, which enables us to monitor the temporal evolution of the multi-layer STMW structure in the RGOS. As the deployment of Argo floats with an oxygen sensor is being expanded, we expect to reveal more detailed spatial–temporal distribution and variability of not only STMW but also OUR. Furthermore, it will be an interesting topic to investigate how the multi-layer STMW structure in the RGOS, which has been maintained during the current LM period, will change after the LM terminates. The southwestward advection of the warm STMW during the current LM period and afterward is also an interesting theme, as the warm STMW formed south of Japan during the previous LM period in 2005 has been reported to be advected to just east of Taiwan (Oka 2009).

Acknowledgements We are grateful to the captain, crew, and scientists onboard the KS-21-9 cruise of the *R/V Shinsei-maru*. The authors also thank Toshio Suga, Shigeki Hosoda, Yoshimi Kawai, Fumiaki Kobashi, Katsuya Toyama, Yuichiro Kumamoto, Naohiro Kosugi, Daisuke Sasano, Masao Ishii, and the two anonymous reviewers for helpful comments. Comments from participants at the research meeting on Air–Sea Interaction, as a part of the Collaborative Research Program of

HyARC, Nagoya University, were helpful. This work was supported by the Ministry of Education, Culture, Sports, Science, and Technology, Japan (Grants-in-Aid for Scientific Research on Innovative Areas under Grant Nos. JP19H05700 and JP19H05704).

Funding Open access funding provided by The University of Tokyo.

Data availability The data presented in this paper are available from the corresponding author upon request.

Open Access This article is licensed under a Creative Commons Attribution 4.0 International License, which permits use, sharing, adaptation, distribution and reproduction in any medium or format, as long as you give appropriate credit to the original author(s) and the source, provide a link to the Creative Commons licence, and indicate if changes were made. The images or other third party material in this article are included in the article's Creative Commons licence, unless indicated otherwise in a credit line to the material. If material is not included in the article's Creative Commons licence and your intended use is not permitted by statutory regulation or exceeds the permitted use, you will need to obtain permission directly from the copyright holder. To view a copy of this licence, visit <http://creativecommons.org/licenses/by/4.0/>.

References

- Akima H (1970) A new method of interpolation and smooth curve fitting based on local procedures. *J Assoc Comput Math* 17:589–602
- Belkin I, Foppert A, Rosby T, Fontana S, Kincaid C (2020) A Double-thermostad warm-core ring of the gulf stream. *J Phys Oceanogr* 50:489–507. <https://doi.org/10.1175/JPO-D-18-0275.1>
- Billheimer SJ, Talley LD, Martz TR (2021) Oxygen seasonality, utilization rate, and impacts of vertical mixing in the Eighteen Degree Water region of the Sargasso Sea as observed by profiling biogeochemical floats. *Global Biogeochem Cycles*. <https://doi.org/10.1029/2020GB006824>
- de Boyer MC, Madec G, Fischer AS, Lazar A, Iudicone D (2004) Mixed layer depth over the global ocean: an examination of profile data and a profile-based climatology. *J Geophys Res* 109:C12003. <https://doi.org/10.1029/2004JC002378>
- Feely RA, Sabine CL, Schlitzer R, Bullister JL, Mecking S, Greeley D (2004) Oxygen utilization and organic carbon remineralization in the upper water column of the Pacific Ocean. *J Oceanogr* 60:45–52. <https://doi.org/10.1023/B:JOCE.0000038317.01279.a>
- Goes M, Christophersen J, Dong S, Goni G, Baringer MO (2018) An updated estimate of salinity for the atlantic ocean sector using temperature–salinity relationships. *J Atmospheric Ocean Technol* 35:1771–1784
- Hanawa K, Sugimoto S (2004) “Reemergence” areas of winter sea surface temperature anomalies in the world’s oceans. *Geophys Res Lett*. <https://doi.org/10.1029/2004GL019904>
- Jenkins W (1980) Tritium and ^3He in the Sargasso Sea. *J Mar Res* 38:533–569
- Kawabe M (1995) Variations of current path, velocity, and volume transport of the Kuroshio in relation with the large meander. *J Phys Oceanogr* 25:3103–3117
- Liu C, Xie S-P, Li P, Xu L, Gao W (2017) Climatology and decadal variations in multicore structure of the North Pacific subtropical mode water. *J Geophys Res Oceans* 122:7506–7520. <https://doi.org/10.1002/2017JC013071>
- Liu C, Xu L, Xie S-P, Li P (2019) Effects of anticyclonic eddies on the multicore structure of the North Pacific subtropical mode water based on Argo observations. *J Geophys Res Oceans* 124:8400–8413

- Lixiao Xu, Xie S-P, Liu Q, Liu C, Li P, Lin X (2017) Evolution of the North Pacific subtropical mode water in anticyclonic eddies. *J Geophys Res Oceans* 122:10118–10130
- Marshall J, Andersson A, Bates N, Brown W, Dewar W, Doney S, Fratantoni D, Joyce T, Straneo F, Toole J, Weller R, Edson J, Gregg M, Kelly K, Lozier S, Palter J, Lumpkin R, Samelson R, Skillingstad E, Silverthorne K, Talley L, Thomas L (2009) The CLIMODE field campaign: observing the cycle of convection and restratification over the Gulf Stream. *Bull Amer Meteor Soc* 90:1337–1350. <https://doi.org/10.1175/2009BAMS2706.1>
- Masuzawa J (1969) Subtropical mode water. *Deep-Sea Res* 16:463–472
- Newman M, Alexander MA, Ault TR, Cobb KM, Deser C, Di Lorenzo E, Mantua NJ, Miller AJ, Minobe S, Nakamura H, Schneider N, Vimont DJ, Phillips AS, Scott JD, Smith CA (2016) The Pacific decadal oscillation. Revisited *J Clim* 29(12):4399–4427. <https://doi.org/10.1175/JCLI-D-15-0508.1>
- Nishikawa S, Tsujino H, Sakamoto K, Nakano H (2010) Effects of mesoscale eddies on subduction and distribution of Subtropical Mode Water in an eddy-resolving OGCM of the western North Pacific. *J Phys Oceanogr* 40:1748–1765
- Nishiyama K, Konaga S, Ishizaki H (1980) Warm water regions off Shikoku associated with the Kuroshio meander (in Japanese with English abstract). *Pap Meteor Geophys* 31:43–52. <https://doi.org/10.2467/mripapers.31.43>
- Nishiyama K, Konaga S, Ishizaki H (1981) Some considerations on the Kuroshio meander and the surrounding oceanographic conditions (in Japanese with English abstract). *Pap Meteor Geophys* 32:109–117. <https://doi.org/10.2467/mripapers.32.109>
- Oka E (2009) Seasonal and interannual variation of North Pacific Subtropical Mode Water in 2003–2006. *J Oceanogr* 65:151–164
- Oka E, Qiu B (2012) Progress of North Pacific mode water research in the past decade. *J Oceanogr* 68:5–20. <https://doi.org/10.1007/s10872-011-0032-5>
- Oka E, Suga T (2003) Formation region of North Pacific subtropical mode water in the late winter of 2003. *Geophys Res Lett*. <https://doi.org/10.1029/2003GL018581>
- Oka E, Suga T (2005) Differential formation and circulation of North Pacific Central Mode Water. *J Phys Oceanogr* 35:1997–2011
- Oka E, Talley LD, Suga T (2007) Temporal variability of winter mixed layer in the mid- to high-latitude North Pacific. *J Oceanogr* 63:293–307. <https://doi.org/10.1007/s10872-007-0029-2>
- Oka E, Suga T, Sukigara C, Toyama K, Shimada K, Yoshida J (2011) “Eddy resolving” observation of the North Pacific Subtropical Mode Water. *J Phys Oceanogr* 41:666–681
- Oka E, Nishikawa H, Sugimoto S, Qiu B, Schneider N (2021) Subtropical Mode Water in a recent persisting Kuroshio large-meander period: part I—formation and advection over the entire distribution region. *J Oceanogr* 77:781–795
- Qiu B, Chen S (2021) Revisit of the Occurrence of the Kuroshio Large Meander South of Japan. *J Phys Oceanogr* 51:3679–3694. <https://doi.org/10.1175/JPO-D-21-0167.1>
- Qiu B, Hacker P, Chen S, Donohue KA, Watts DR, Mitsudera H, Hogg NG, Jayne SR (2006) Observations of the subtropical mode water evolution from the Kuroshio extension system study. *J Phys Oceanogr* 36:457–473
- Stommel HS (1947) Note on the use of the T-S correlation for the dynamic height anomaly computations. *J Mar Res* 2:85–92
- Suga T, Hanawa K (1990) The mixed layer climatology in the northwestern part of the North Pacific subtropical gyre and the formation area of Subtropical Mode Water. *J Mar Res* 48:543–566
- Suga T, Hanawa K (1995a) The subtropical mode water circulation in the North Pacific. *J Phys Oceanogr* 25:958–970
- Suga T, Hanawa K (1995b) Interannual variations of North Pacific Subtropical Mode Water in the 137°E section. *J Phys Oceanogr* 25:1012–1017
- Suga T, Hanawa K, Toba Y (1989) Subtropical mode water in the 137°E section. *J Phys Oceanogr* 19:1605–1618
- Sugimoto S, Hanawa K (2005) Remote reemergence areas of winter sea surface temperature anomalies in the North Pacific. *Geophys Res Lett* 32:L01606. <https://doi.org/10.1029/2004gl021410>
- Sugimoto S, Hanawa K (2014) Influence of Kuroshio path variation south of Japan on formation of subtropical mode water. *J Phys Oceanogr* 44:1065–1077
- Taneda T, Suga T, Hanawa K (2000) Subtropical mode water variation in the northwestern part of the North Pacific subtropical gyre. *J Geophys Res* 105:19591–19598. <https://doi.org/10.1029/2000JC900073>
- Uehara H, Suga T, Hanawa K, Shikama N (2003) A role of eddies in formation and transport of North Pacific Subtropical Mode Water. *Geophys Res Lett*. <https://doi.org/10.1029/2003GL017542>
- Weiss RF (1970) The solubility of nitrogen, oxygen and argon in water and seawater. *Deep Sea Res Oceanogr* 17:721–735. [https://doi.org/10.1016/0011-7471\(70\)90037-9](https://doi.org/10.1016/0011-7471(70)90037-9)
- Xie T, Newton R, Schlosser P, Guo L, Wang L, Huang T, Li Y, Wang Z, Dai M (2021) Apparent oxygen utilization rates based on tritium-helium dating in the South China Sea: Implications for export production. *Deep Sea Res*. <https://doi.org/10.1016/j.dsr.2021.103620>
- Xu L, Li P, Xie S-P, Liu Q, Liu C, Gao W (2016) Observing mesoscale eddy effects on mode-water subduction and transport in the North Pacific. *Nat Commun* 7:10505. <https://doi.org/10.1038/ncomms10505>
- Yasuda T, Hanawa K (1997) Decadal changes in the mode waters in the midlatitude north pacific. *J Phys Oceanogr* 27:858–870. [https://doi.org/10.1175/1520-0485\(1997\)027%3c0858:DCITMW%3e2.0.CO;2](https://doi.org/10.1175/1520-0485(1997)027%3c0858:DCITMW%3e2.0.CO;2)